Numerical investigation of heat transfer enhancement about a thermally isolated body: outcome of Hartmann and Reynolds numbers

M. U. Ahammad[1-3], M. M. Rahman[2], and M. L. Rahman[3]

[1]Department of Mathematics, Dhaka University of Engineering and Technology (DUET), Gazipur-1700, Bangladesh

[2]Department of Mathematics, Bangladesh University of Engineering and Technology (BUET), Dhaka-1000, Bangladesh

[3]Department of Mathematics, Rajshahi University, Rajshahi-6205, Bangladesh

---

ABSTRACT: In this paper, coupled flow and heat transfer by combined convection in a laminar, incompressible, electrically conducting fluid-filled two-dimensional cavity with a thermally isolated body has been analyzed. The developed mathematical model is governed by the conservation of mass, momentum and energy equations and the problem is solved numerically. The effects of two physical parameters namely the Hartmann number *Ha* and the Reynolds number *Re* on the flow and heat transfer are discussed and exposed though graphs and tables. The phenomenon inside the cavity for the mentioned parameters is studied through streamline and isotherm patterns. Moreover average Nusselt number which is the representative of heat transfer rate at hot wall is calculated. It is observed that the rate of heat transfer at the bottom heated surface increases with a decrease in *Ha*, where as it shows reverse effect in case of the *Re*.

KEYWORDS: Hartmann number, Heat transfer enhancement, Reynolds number, Thermally isolated.

1 INTRODUCTION

The MHD combined convection and heat transfer in cavity has been studied extensively and is reasonably well-understood. It plays a significant role in controlling the rate of heat transfer as well as temperature distribution. In addition, the enclosure ventilated geometry has been widely considered in heat transfer for the reason of its fundamental importance and its many applications, including electronic equipment cooling, heat exchangers, solar thermal collector systems and thermal environmental control of dwellings etc. The most significant features occur in the context of MHD heat transfer is the existence of Lorentz force rising due to the imposition of magnetic field that changes the heat transport phenomena. Model studies of the above phenomena of MHD mixed convection have been made by many authors. Billah et al. [1] carried out aspect ratio and prandtl number effect on MHD mixed convection heat transfer enhancement in a lid-driven enclosure having a heat-generating body. Gau et al. [2] performed an experimental study on mixed convection in a horizontal rectangular channel that was heated from a side. Rahman et al. [3] performed the combined forced and natural convection problem in a ventilated square cavity containing a heat conducting horizontal circular cylinder. Huang and Li [4] calculated heat transfer enhancement of free surface MHD-flow by the wall with non-uniform electrical conductivity. The authors explained the flow behaviors, heat transfer coefficients, friction factors and pressure drops under different Hartmann numbers in their study. An unsteady laminar combined convection flow and heat transfer of an electrically conducting and heat generating or absorbing fluid-filled vertical lid-driven cavity in the presence of magnetic field has been analyzed by Chamkha [5]. Mehmet and Elif [6] examined the inclination effect of the rectangular enclosure for electrically conducting fluid with a magnetic field in the case of natural convective flow. Abo El-Nasr et al [7] developed heat transfer characteristics of horizontal cylinder cooling under single impinging water jet. Oztop et al. [8] performed the combined convection flow in a lid-driven cavity with a circular body. In their work the left wall of the cavity was kept heated while the right wall was considered as cool and other two walls were insulate. For understanding the effect of Prandtl number a Hydromagnetic mixed convection problem in a double-lid driven cavity with a heat-generating body have been investigated by Rahman et al. [9].

Later on, Rahman et al. [10] studied combined free and forced convection problem in cavity vented with a heat-generating solid circular block and presented the significant role of Reynolds and Prandtl number. Thermal comfort in a room with windows at adjacent walls along with additional vents was studied by Prakash and Ravikumar [11]. Sharif et al. [12] reported the assisting flow behavior of MHD mixed convection inside a ventilated enclosure. Recently, modeling and simulation of MHD convective heat transfer of channel flow having a cavity was analyzed by Munshi et al [13].

The task in this article is to examine the fluid flow patterns along with the enhancement of heat transfer performance from the lower hot surface of the studied geometry so that the average temperature in the system can be kept below the allowable threshold value.

2   PHYSICAL MODEL

A square cavity containing incompressible fluid with a centered insulated obstacle is shown in the Figure 1. The cavity dimensions are defined by L for each side. The bottom wall is heated while the remaining walls are considered perfectly adiabatic. The entrance and outlet of the cavity are positioned at the bottom of the left wall and at the top of the right wall respectively. A magnetic field of strength B_0 is assumed to be applied transversely to the opposite flow direction. The size of each opening is equal to one-tenth of the cavity length. The inflow state is (u_i, T_i) while zero diffusion flux is assumed for outflow.
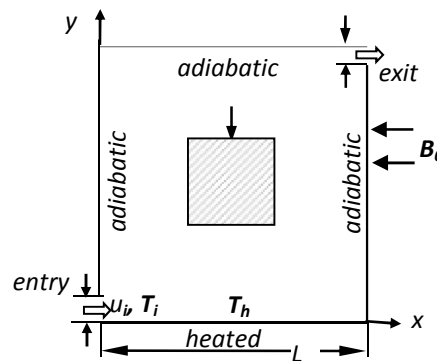
Fig. 1.   Cavity configuration for studied problem

3   MATHEMATICAL ANALYSIS

The studied fluid is treated as laminar, Newtonian and incompressible with the flow in the mixed convection regime. Two-dimensional mass, momentum and energy conservation equations are considered as the governing equations in the present work and under the Boussinesq approximation the equations can be described in vector forms as follows:

$$\underline{\nabla}.\,\underline{q} = 0 \tag{1}$$

$$\left(\underline{q}.\underline{\nabla}\right)\underline{q} = -\frac{1}{\rho}\underline{\nabla}\,p + \upsilon\,\nabla^2\,\underline{q} + \underline{F} \tag{2}$$

$$\left(\underline{q}.\underline{\nabla}\right)T = \alpha\,\nabla^2\,T \tag{3}$$

$$F_x = 0,\; F_y = g\beta\left(T - T_i\right) - \frac{\sigma B_0^2 v}{\rho} \quad \text{are assumed as two components of the body force } \underline{F}.$$

where $\underline{q}$ stands for the velocity vector, $\underline{F}$ is the body force, T denotes the temperature of the fluid, T_i is ambient temperature, v is the kinematics viscosity, α is the thermal diffusivity, p is the pressure, ρ is the density and σ is the electrical conductivity of the fluid.

By introducing the following non-dimensional variables, the above equations are made dimensionless as stated in equations (4)-(7).

$$X = \frac{x}{L}, Y = \frac{y}{L}, U = \frac{u}{u_i}, V = \frac{v}{u_i}, P = \frac{p}{\rho u_i^2}, \theta = \frac{(T - T_i)}{(T_h - T_i)}$$

P is the dimensionless pressure, u_i is the ambient velocity, θ is the dimensionless temperature, T_h is the constant temperature of hot wall of the cavity.

$$\frac{\partial U}{\partial X} + \frac{\partial V}{\partial Y} = 0 \tag{4}$$

$$U\frac{\partial U}{\partial X} + V\frac{\partial U}{\partial Y} = -\frac{\partial P}{\partial X} + \frac{1}{Re}\left(\frac{\partial^2 U}{\partial X^2} + \frac{\partial^2 U}{\partial Y^2}\right) \tag{5}$$

$$U\frac{\partial V}{\partial X} + V\frac{\partial V}{\partial Y} = -\frac{\partial P}{\partial Y} + \frac{1}{Re}\left(\frac{\partial^2 V}{\partial X^2} + \frac{\partial^2 V}{\partial Y^2}\right) + Ri\,\theta - \frac{Ha^2}{Re}V \tag{6}$$

$$U\frac{\partial \theta}{\partial X} + V\frac{\partial \theta}{\partial Y} = \frac{1}{Re\,Pr}\left(\frac{\partial^2 \theta}{\partial X^2} + \frac{\partial^2 \theta}{\partial Y^2}\right) \tag{7}$$

where, the Reynolds number, Prandtl number, Hartmann number, Richardson number are defined respectively as

$$Re = \frac{u_i L}{\upsilon}, \quad Pr = \frac{\upsilon}{\alpha}, \quad Ha = B_0 L\sqrt{\frac{\sigma}{\mu}}, \quad Ri = \frac{Gr}{Re^2}$$

The concerning boundary conditions in the dimensionless form are given below:

At the inlet: $U = 1, V = 0, \theta = 0$

At the outlet: convective boundary condition (CBC), $P = 0$

At the bottom heated surface: $\theta = 1$

At the left, right and top walls: $U = 0, V = 0, \frac{\partial \theta}{\partial N} = 0$

At the surface of the block: $U = 0, V = 0, \frac{\partial \theta}{\partial N} = 0$

The average Nusselt number Nu_{av} at the hot wall is given by $Nu_{\alpha v} = -\int_0^1 \left(\frac{\partial \theta}{\partial Y}\right)dX$

The bulk average fluid temperature in the enclosure is defined as $\theta_{av} = \int \theta \frac{d\overline{V}}{\overline{V}}$, where $\overline{V}$ is the cavity volume.

4 COMPUTATIONAL DETAILS

The solution of the governing equations with boundary conditions are obtained through the Galerkin weighted residual based finite element method. Firstly, the problem is defined as a two dimensional cavity and the solution domain is discretized into finite element meshes, which are composed of non-uniform triangular elements. Applying Galerkin weighted residual technique the governing equations are transferred into a system of integral equations. Boundary conditions are then imposed and the nonlinear equations are transformed into linear algebraic equations with the help of Newton's method which are finally solved by triangular factorization method.

In order to obtain the grid independence solution, a grid refinement study is conducted to select proper grid resolution. Various size of grid having 2024, 3540, 4508, 5554 and 7160 elements are used to determine the average rate of heat

transfer at the heated wall of the cavity. The average heat transfer rate at the hot wall with grid elements is revealed in Table-1 and Figure 2. As it is seen that there is no significant discrepancy ahead of 5554 elements, all computations are performed using this grid resolution.

Table 1.   Average Nusselt number for different grid elements while Ri = 1.0, Ha = 10.0, D = 0.2, Re = 100 and Pr = 0.71

Elements	Nu_{av}	Discrepancy (%)
2024	6.201839	---
3540	6.202839	0.02
4508	6.212839	0.17
5554	6.213839	0.19
7160	6.213939	0.19

The solution procedure has been validated against the numerical results of Oztop et al. [8] shown in the Figure 3. This figure shows that the streamline and isotherm patterns in the present work have excellent agreement with those obtained by Oztop et al. [8]. Thus the numerical code used in this analysis can perform the present problem with logical agreement.
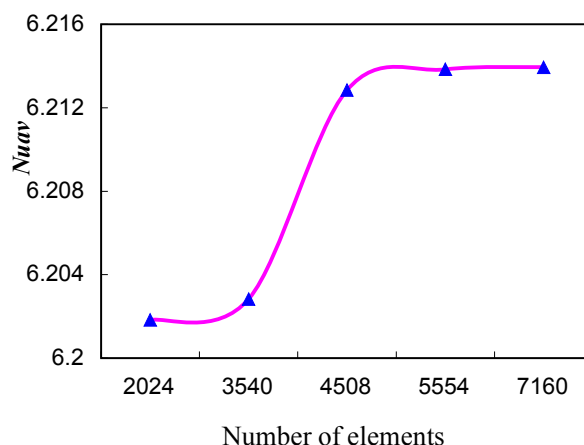
Fig. 2.   Average Nusselt number for different grid elements
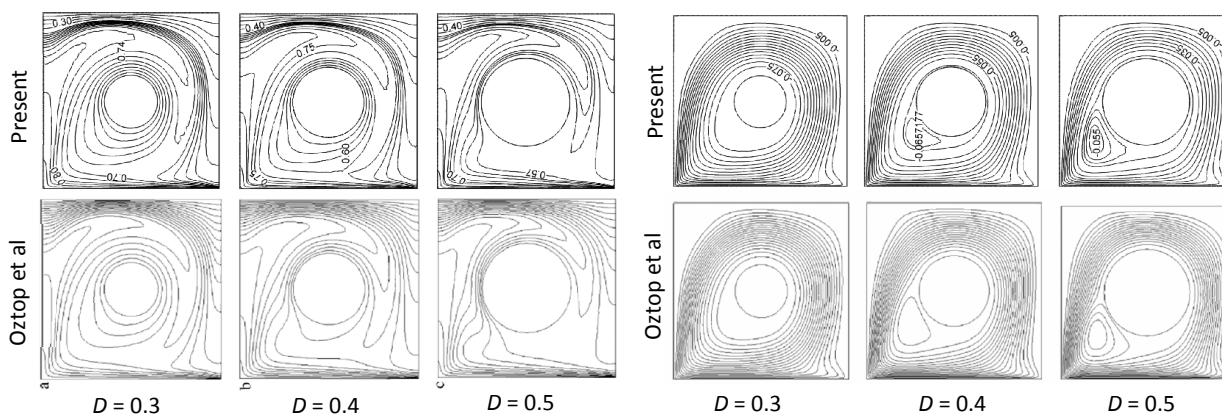
Fig. 3.   Comparison of streamlines (left) and isotherms (right) between the work of Oztop et al. [8] and present while Gr = 10^5, Pr = 0.71, C = 0.5 and Re = 1000

5   RESULT AND DISCUSSIONS

In this section, among the related parameters of the current problem the impacts of two controlling parameters namely Hartmann number *Ha* and Reynolds number *Re* on the streamlines and isotherms are executed. The considered values of

Hartmann number and Reynolds number are Ha = (0, 20, 50, 100) and Re = (50, 200, 350, 500) while the other parameters Pr, D, are kept fixed 0.71, 0.2 respectively.
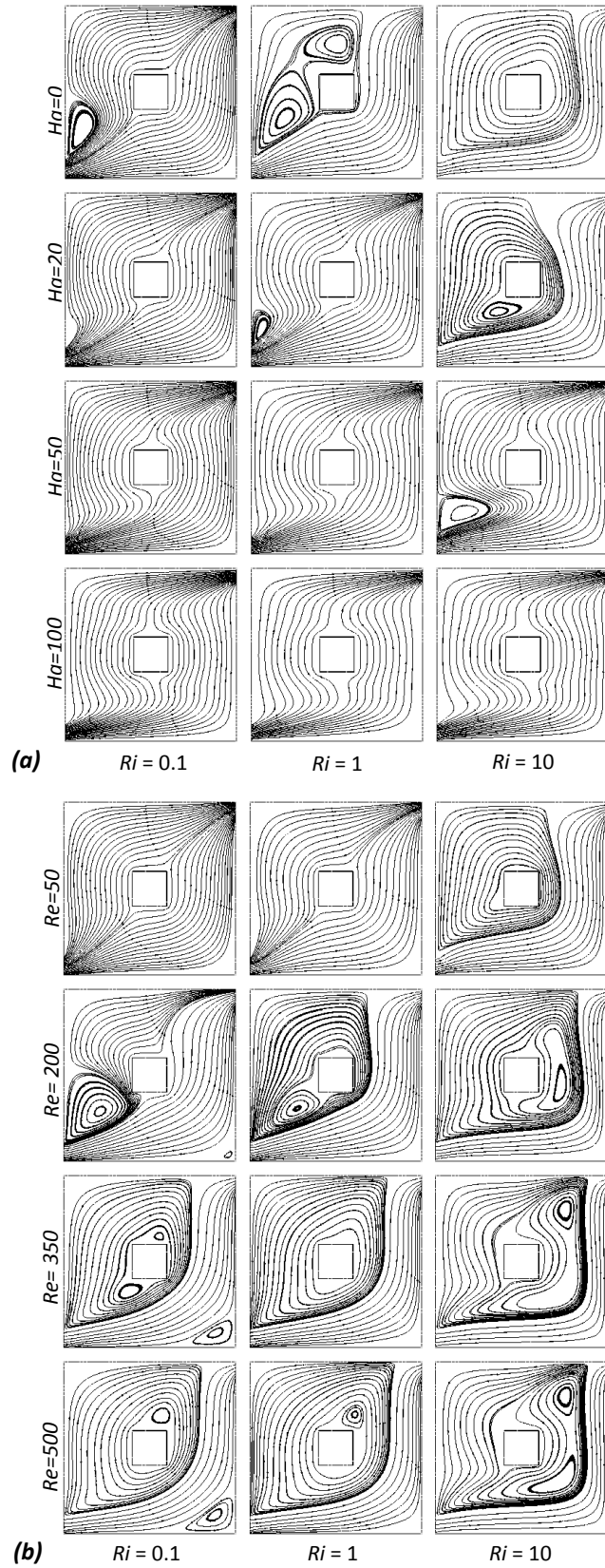
Fig. 4. *Streamlines for various (a) Hartmann number and (b) Reynolds number with Richardson number in the range 0.1 $\leq Ri \leq$ 10*
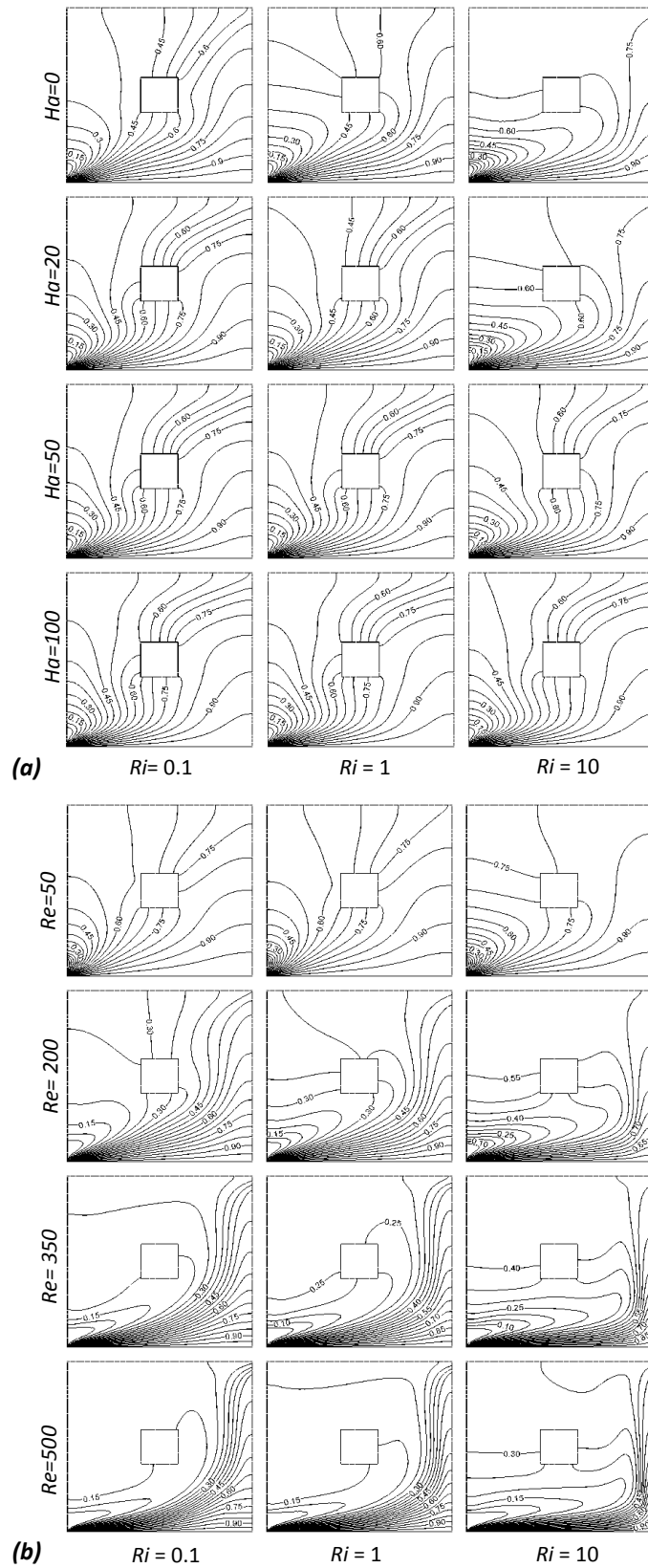
Fig. 5. *Isotherms for various (a) Hartmann number and (b) Reynolds number with Richardson number in the range 0.1 ≤ Ri ≤ 10*

The mixed convection parameter Ri is varied in the range of 0.1 to 10. The outcomes of the present study are discussed here in three steps in order to focus the characteristic of flow field, temperature distribution inside the ventilated cavity as well as overall heat transfer including average Nusselt number at the bottom wall and average temperature of the cavity fluid.

5.1 FLOW FEATURES

Figure 4(a) depicts the effects of the magnetic field parameter on streamlines at different Richardson number. At low Hartmann number $Ha = 0$, a rotating cell is created just above the inlet in the domain $Ri = 0.1$ and it increases rapidly for the consecutive value of $Ri = 1$. On the other hand it is followed that for the above two convective regimes of Richardson number the flow structures are almost identical at the rest three considered values of Ha (= 20, 50, 100). Interestingly, in the dominant free convection domain the patterns of the cavity flow change dramatically for the cases of lower Ha than that of higher value of Ha. The reality established here is that the application of transverse magnetic field acting as Lorentz's force which retards the flow. As expected, the flow strength is reduced with increasing the Hartmann number.

A general observation concerning the influence of Reynolds number on streamlines has been demonstrated in Figure 4(b). In the dominant and pure mixed convection region the flow patterns inside the enclosure appear as an onion shape that elongated from the entry to the exit port at Re=50, while a large anti-clockwise rotating cell formed occupying the centered block for the case $Ri = 10$. When $Re = 200$, a vortex is seen near the lower left side of the cavity, consequently open lines shrinks towards the obstacle at $Ri = 0.1$ and this vortex enlarges very fast as Ri increases. For higher values of $Re = 350$, 500 the vortices expand in size and small eddies and these are nearly similar in all the ranges of $0.1 \le Ri \le 10$. This figure is also indicating that the Reynolds number is an effective parameter on streamlines.

5.2 THERMAL FIELDS

The inspection of the heatlines profile relating to these various values of the Hartmann number are illustrated in Figure 5(a). The isothermal lines are scattered through all over the enclosure for the choosing values of four Hartmann number as $Ha = 0$, 20, 50, 100 in the different values of Richardson number regimes with the exception of two cases. However a significant change is found for the lowest value of $Ha = 0$ that is, in the absence of magnetic field parameter along with $Ri = 10$. Also a noticeable variation is observed in the dominant natural convective domain at $Ha = 20$. It is seen that heatlines are crowded at the bottom wall near the inlet port and a boundary layer is created at the vicinity of the heated surface of the cavity for each case.

In order to clearly exhibit the thermal field characteristic of the working area for the different Reynolds number the corresponding isotherms are displayed in Figure 5(b). At smaller value of Reynolds number ($Re = 50$) temperature distribution inside the cavity shows non-linearity for all the values of Ri varies as 0.1-10 with a minor change in $Ri = 10$. In the dominant forced convection and pure mixed convection area it can be easily followed that isotherms are shrink gradually in the direction of bottom-right sided wall with the increasing values of Reynolds number from 200 to 500 as the basis of higher Re more suppression. In addition, for these three values of Reynolds number the tendency of heatlines minimization is more visible in the case of $Ri = 10$ and some folding isotherms are returned to the left wall.
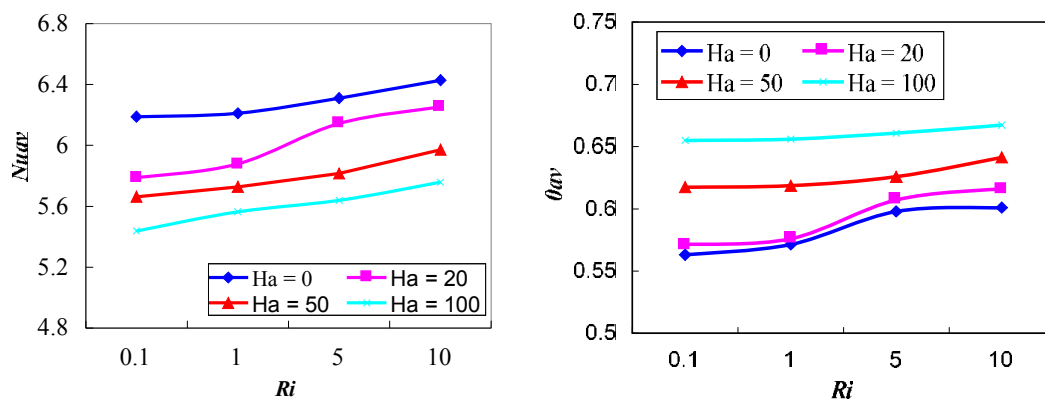
Fig. 6. *Average Nusselt number and average fluid temperature versus Richardson number for different values of Hartman number*
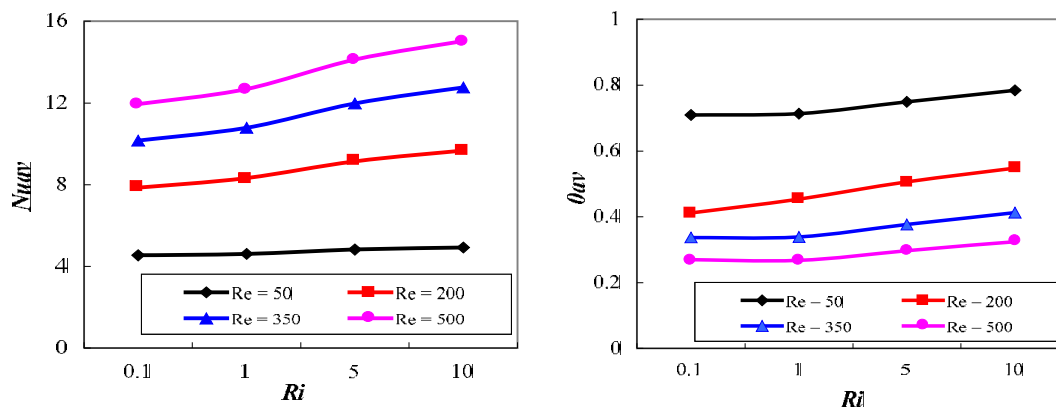
Fig. 7. *Average Nusselt number and average fluid temperature versus Richardson number for different values of Reynolds number*

5.3   HEAT TRANSFER

At last the heat transfer efficiency of the enclosure for the two above discussed parameters are presented in terms of average Nusselt number Nu_{av} and the dimensionless average bulk temperature θ_{av}. Figure 6 plots the variation of both average Nusselt number and average fluid temperature for different values of Hartmann number. The variation profile indicates that heat transfer rate decreases as the value of Ha increases within the range of $0.1 \leq Ri \leq 10$ and so an opposite result is found for the average fluid temperature in the cavity. The higher the Hartmann number the smaller are the fluctuations in the average temperature.

To show the effect of Reynolds number, Figure 7 records the variations of Nu_{av} and θ_{av} as the function of Ri within range of 0.1–10 for different values of Re. It is evident that average Nusselt number increases with the increase in Reynolds number Re, where as it shows reverse effect in the case of average temperature of cavity fluid.

Tables 2 and 3 show the heat transfer variation at the heated wall of the enclosure through the average Nusselt number for the different values of Ha and Re in that order. Results clearly give an idea about how the aforementioned parameters affect the thermal performance in the enclosure, and how the aforesaid parameters are significant on the overall heat transfer process across the enclosure.

Table 2. *Variation of average Nusselt number (Nu_{av}) with Hartmann number Ha*

Ri	*Ha = 0*	*Ha = 20*	*Ha = 50*	*Ha = 100*
0.1	6.189092	5.788497	5.663728	5.438015
1.0	6.211818	5.878837	5.728370	5.564770
5.0	6.310872	6.145266	5.816642	5.639284
10.0	6.429270	6.252779	5.97306	5.758791

Table 3. *Variation of average Nusselt number (Nu_{av}) with Reynolds number Re*

Ri	*Re = 50*	*Re = 200*	*Re = 350*	*Re = 500*
0.1	4.542412	7.851059	10.16379	11.93755
1.0	4.610437	8.320327	10.78297	12.69044
5.0	4.822014	9.143034	11.97443	14.12518
10.0	4.921946	9.671546	12.76067	15.03054

6   CONCLUSION

Two pertinent parameters of this article have provided some reliable information on the condition of the cavity vented flow and heat transfer. From the present investigation it is seen that for different Hartmann number *Ha* with fixed Reynolds number *Re* and Prandtl number *Pr*, heat transfer rate at the hot wall of the cavity is larger for smaller value of *Ha*. But an opposite effect is noticed for the case of different Reynolds number *Re* while Hartmann number *Ha* and Prandtl number *Pr* are kept stationary; that is, heat transfer enhanced as *Re* increases. In addition, the flow and thermal fields in the case of Reynolds number are much affected than that of Hartmann number. Thus the considered parameters in this study can be treated as heat transfer controlling parameter and it is observed that Hartmann number and Reynolds number is an important factor for the enhancement of heat transfer.

REFERENCES

[1] J Billah M. M., Rahman M. M., Ahamed J. U., and Bhuiya M. M. K., "MHD mixed convection heat transfer enhancement in a lid-driven enclosure having a heat-generating body: aspect ratio and prandtl number effect," *International Journal of Energy & Technology*, vol. 3(13), pp. 1–8, 2011.

[2] Gau C., Jeng Y.C., and Liu C.G., "An experimental study on mixed convection in a horizontal rectangular channel heated from a side," *ASME J. Heat Transfer*, vol. 122, pp. 701-707, 2000.

[3] Rahman M.M., Alim M.A., Saha S., and Chowdhury M.K., "Mixed convection in a vented square cavity with a heat conducting horizontal solid circular cylinder," *Journal of Naval Architecture and Marine Engineering*, vol. 5(2), pp. 37-46, 2008.

[4] Huang H. L.and Li B., "Heat transfer enhancement of free surface MHD-flow by the wall with non-uniform electrical conductivity,". *International Journal of Energy and Environment*, vol. 1(6), pp. 1027-1038, 2010.

[5] Chamkha A.J., "Hydro magnetic combined convection flow in a vertical lid-driven cavity with internal heat generation or absorption," *Numer. Heat Transfer Part A*, vol. 41, pp. 529-546, 2002.

[6] Mehmet C.E. and Elif B., "Natural convection flow under a magnetic field in an inclined rectangular enclosure heated and cooled on adjacent walls," *Fluid Dynamics Research*, vol. 38, pp. 564-590, 2006.

[7] Abo El-Nasr M. M., Abidou M. A., and Hussein H. A., "Heat transfer characteristics of horizontal cylinder cooling under single impinging water jet," *International Journal of Applied Sciences and Engineering Research*, vol. 1(2), pp. 287-301, 2012.

[8] Oztop H.F., Zhao Z., and Yu B., "Fluid flow due to combined convection in lid-driven enclosure having a circular body," *Int. J. Heat and Fluid Flow*, vol. 30, pp. 886-901, 2009.

[9] Rahman M.M, Nasrin R., and Billah M.M., "Effect of Prandtl number on hydromagnetic mixed convection in a double-lid driven cavity with a heat-generating obstacle," *Engineering e-Transaction*, vol. 5(2), pp. 90-96, 2010.

[10] Rahman M.M., Parvin S., Rahim N.A., Islam M.R., Saidur R., and Hasanuzzaman M., "Effects of Reynolds and Prandtl number on mixed convection in a ventilated cavity with a heat-generating solid circular block," *Applied Mathematical Modelling*, vol. 36, pp. 2056–2066, 2012.

[11] Prakash D. and Ravikumar P., "Study of thermal comfort in a room with windows at adjacent walls along with additional vents," *Indian Journal of Science and Technology*, vol. 6(6), pp. 4659-4669, 2013.

[12] Sharif U.M., Rahman M.M., Saklayen M.A., Billah M.M., and Elias M., "A numerical study of assisting MHD mixed convection inside a ventilated cavity," *Engineering e-Transaction*, vol. 7(1), pp. 6-13, 2012.

[13] Munshi M.J.H., Azad A.K., Begum R.A., Uddin M.B. and Rahman M.M., "Modeling and Simulation of MHD convective heat transfer of channel flow having a cavity" *International Journal of Mechanical and Materials Engineering*, vol. 8(1), pp. 63-72, 2013.

[14] Reddy J.N., An Introduction to Finite Element Analysis. *McGraw-Hill*, 1993.